Energy loss and fragmentation of 3 keV C60+ ions at grazing scattering from a KCl(0 0 1)

Kimura, Kenji; Matsushita, T.; Nakajima, K.; Suzuki, M.

Energy loss and fragmentation of 3-keV C_{60}^{+} ions at grazing scattering from a KCl(001)

K. Kimura*, T. Matsushita, K. Nakajima, M. Suzuki

Department of Micro Engineering, Kyoto University, Yoshida-honmachi, Sakyo, Kyoto 606-8501, Japan

Charge state, angular and energy distributions of reflected projectiles are measured when 3 keV $C_{60}^{+, 2+}$ ions are scattered from a clean and flat KCl(001) surface under grazing incidence. The dominant charge state is found to be C_{60}^{+} irrespective of the incident charge state as is expected by the electronic structure of KCl and C_{60} ions. The observed angular distribution has a well defined peak at a specular angle, indicating that the normal energy is not dissipated during the grazing angle scattering. In spite of no dissipation of the normal energy we observe the fragmentation of the scattered C_{60}^{+} ions. The energy transferred from the parallel energy to the internal excitations was estimated from the observed fragment distribution. The transferred energy changes from almost 0 eV to ~ 15 eV when the angle of incidence changes from 1 º to 6 º, which is less than 10% of the observed energy loss of the C_{60}^{+} ions.

PACS: 79.20.Rf, 78.30.Na, 34.50.Bw, 79.60.Bm

*corresponding author: Tel: +81-75-753-5253; Fax: +81-75-753-5253; E-mail: kimura@kues.kyoto-u.ac.jp

1. Introduction

The interactions of ions with surfaces have been extensively studied for the past two decades. Considerable progress has been achieved on the understanding of the ion-surface interactions, such as charge exchange, energy loss, secondary particle emission, using grazing angle scattering of ions from surfaces [1]. Compared to atomic ions, however, the interaction of molecular/cluster ions with surfaces were rarely studied. The interesting aspect of the cluster-surface interaction is the internal degree of freedom. The internal excitations may play an important role during ion-surface scattering. When a cluster ion impinge on the surface, however, the cluster ion easily shatter into fragment ions. As a result, it is difficult to observe the role of the internal excitations in the ion-surface interaction.

Regarding the fragility of the cluster ions, the Buckminster fullerene ion C_{60}^+ is unusually stable against surface impacts [2, 3]. Monte Carlo simulations for C_{60} impact on a structureless potential wall showed that there is a threshold impact energy of ~ 150 eV for fragmentation of C_{60} [4]. This threshold energy corresponds to the grazing angle of incidence $\theta_i = 7°$ for 10 keV C_{60}^+, indicating that keV C_{60}^+ ions can be reflected from a surface without fragmentation under grazing incidence. A recent study, however, showed that the fragmentation of C_{60}^+ occurs via delayed C_2 emission when keV C_{60}^+ ions are incident on a clean and flat Al(001) surface at $\theta_i = 1 - 3°$ [5]. It was shown that the kinetic energy for the motion along the surface normal (normal energy) is efficiently transferred to internal excitations of C_{60}^+, and the internal excitations cause the delayed C_2 emission. We have also observed fragmentation of C_{60}^+ when 3 keV C_{60}^+ ions are incident on KCl(001) surface at $\theta_i = 1 - 5°$ [6]. In this case, however, we did not observe dissipation of the normal energy. The possible source of the internal excitations is therefore the kinetic energy for the motion parallel to the surface (parallel energy), although the mechanism of energy transfer from the parallel energy to the internal excitations was not clarified. In the present paper, we extend our previous study and discuss the energy transfer from the parallel motion to the internal excitations during grazing angle scattering of 3 keV C_{60}^+ ions from KCl(001).

2. Experimental

A single crystal of KCl was cleaved in air and mounted on a 5 axis precision goniometer in an ultra high vacuum chamber (base pressure 2×10^{-10} Torr). The surface of KCl(001) was heated at 300 ºC for several hours to prepare a clean surface [7] and kept at 250 ºC during the measurements to prevent surface charging [8]. Powder of C_{60} was evaporated in a small oven installed in a 10-GHz ECR ion source. The ions extracted from the ion source were mass separated by a double focusing 90º sector magnet. The separated $C_{60}^{+, 2+}$ ion beam was collimated to less than 0.5×0.5 mm^2. The beam was guided into the UHV chamber via a differential pumping system and incident on KCl(001) at a grazing angle $\theta_i = 1 – 5$º.

The angular distributions of the reflected particles were measured by a two-dimensional position-sensitive detector (2D-PSD) consisting of micro channel plates and a resistive anode. The diameter of 2D-PSD was 40 mm and it was placed 160 mm downstream of the target KCl crystal. The 2D-PSD was equipped with a pair of electric field plates, which allowed to measure charge state distributions of the reflected particles.

The energy spectra of the reflected ions were also measured by a cylindrical electrostatic analyzer (CEA). The CEA was placed 100 mm downstream of the target KCl crystal and was able to rotate around the target. The measured energy resolution of the CEA was better than 0.25%.

3. Results and discussion

3.1. Charge state distribution

Figure 1 shows an example of the scattering angle distribution of the reflected particles when 3 keV C_{60}^+ ions are incident on KCl(001). There are three well defined peaks. The sharp peak on the left hand side is the residual incident beam. The reflected particles are separated into two peaks corresponding to C_{60}^+ and C_{60}^0 by means of the electric field plates. The most striking feature seen in this figure is the negligibly small fraction of C_{60}^0 [9]. Figure 2 shows the observed C_{60}^+ fraction as a function of θ_i. In contrast with the recent study on the grazing angle scattering of 5 – 25 keV C_{60}^+ from Al(001) [5], where C_{60}^+ fraction was less than 4%, the C_{60}^+ fraction is dominant in the present case. For comparison,

we also measured the charge state distributions of reflected 3 keV C_{60}^{2+} ions under grazing incidence. The observed C_{60}^{+} fractions are shown by open circles in Fig. 2. The observed C_{60}^{+} fraction is almost the same as the case of C_{60}^{+} incidence and there is no C_{60}^{2+} observed. The small difference between the C^{+} and C^{2+} incidences is attributed to the image acceleration. These results can be explained by the electronic structures of KCl and C_{60} ions. While the ionization energy of C_{60}^{+} (11.4 eV) coincides with the Cl 3p band, the ionization energy of C_{60} (7.6 eV) locates in the band gap of KCl [10]. As a result, slow C_{60}^{2+} ions are almost completely neutralized via resonant neutralization process in front of KCl(001). For C_{60}^{+} ions, however, both resonant and Auger neutralization processes are not allowed. Thus, C_{60}^{+} is dominant irrespective of the incident charge state. This situation is very suitable to study energy loss of C_{60}^{+}, because a simple CEA can be used for precise measurements of energy spectra of reflected C_{60}^{+}.

3.2. Scattering angle distribution

Figure 3 shows the observed most probable scattering angles of C_{60}^{+} (open circles) and C_{60}^{0} (solid circles) as a function of the incident angle θ_i for the grazing angle scattering of 3 keV C_{60}^{+}. The dashed line indicates the specular reflection. All data points of C_{60}^{+} fall on this line, showing that the 3 keV C_{60}^{+} ions are specularly reflected from KCl(001) at θ_i at least up to 4.6º which corresponds to the normal energy, $E_{\perp}$, of 20 eV. Small angular shifts towards larger scattering angles observed for C_{60}^{0} might be attributed to the image acceleration [6, 11]. For comparison, the scattering angles observed for the grazing angle scattering of 3 keV C_{60}^{2+} are also shown by triangles in Fig. 3. The reflected particles appear at scattering angles slightly larger than the specular angle. The deviation from the specular angle is larger than that of the C_{60}^{+} incidence as is expected from the image acceleration. Summarizing the observation of the scattering angle distribution, the normal energy of 3 keV C_{60}^{+} ion is not dissipated during the grazing angle scattering from KCl(001) when $E_{\perp} < 20$ eV.

The present result is different from the recent observation of the grazing angle scattering of 2.5 – 62.5 keV C_{60}^{+} from Al(001) reported by Welthekam and Winter [5]. They

observed that the C_{60}^+ ions were subspecularly reflected from Al(001) at $E_\perp$ larger than 5 – 7 eV while the C_{60}^+ ions were reflected almost specularly at $E_\perp$ smaller than 5 - 7 eV. This behavior was qualitatively reproduced by their MD simulation, although the critical normal energy for the specular reflection predicted by the MD simulation (15 - 20 eV) is several times larger than the observed value (5 – 7 eV). From the MD simulation, the origin of the subspecular reflection was attributed to the internal excitations of C_{60}^+ during scattering, i.e. the normal energy is efficiently transferred to the internal excitations upon reflection. Similar subspecular reflection was also observed for C_{60}^+ scattering from HOPG surfaces at θ_i = 15 º [12]. The observed most probable scattering angle changed from 13.5 to 5 º when the incident energy changed from 0.5 to 5 keV (corresponding $E_\perp$ are 33.5 – 335 eV). This behavior was also reproduced by MD simulation and the dissipated normal energy was found to be used for the deformation of the surface atomic plane during scattering. For a diamond surface, however, MD simulation showed specular reflection under analogous conditions [12], indicating that the scattering behavior of C_{60}^+ strongly depends on the target surface. In the present case, the normal energy is not dissipated even at $E_\perp$ = 20 eV (3 keV C_{60}^+ at θ_i = 4.6 º).

3.3. Energy loss

Figure 4 shows examples of the observed energy spectra of the specularly reflected 3 keV C_{60}^+. The spectrum has a sharp peak at energies slightly lower than the incident energy when θ_i is small. With increasing θ_i, the peak shifts toward lower energies and additional small peaks appear in the low energy side of the first peak. The number and the intensities of these additional peaks increase with θ_i. These peaks are almost equally separated by ~ 106 eV irrespective of θ_i. These multi-peak structures can be ascribed to neither skipping motion [13] nor subsurface channeling [14]. Because the multi-peak structure becomes more pronounced with increasing θ_i, which is opposite to what expected for either skipping or subsurface channeling.

A possible origin of the observed multi-peak structure is the fragmentation of C_{60}^+. As was mentioned above, the normal energy was transferred to the internal excitations when

C_{60}^+ ions were incident on Al(001) under grazing incidence and the resulting fragmentation of C_{60}^+ via a sequential C_2-loss process was actually observed [5]. The C_2 fragments carry ~1/30 of the kinetic energy of C_{60}^+, which is in agreement with the observed peak separation. In order to confirm this explanation, energy spectra were measured at different incident energies. The observed energy spectra are shown in Fig. 5. The spectra show the multi-peak structures similar to Fig. 4. The observed peak separations were ~ 36 and ~ 69 eV at 1 and 2 keV, respectively. These values are again close to 1/30 of the kinetic energies of the C_{60}^+ ions, confirming that the observed peaks correspond to the C_{60-2n}^+ ions produced by the sequential C_2-loss process. This is somewhat surprising, because the normal energy is not transferred to the internal excitation in the present case. Considering the activation energy for C_2 loss (~ 10 eV for C_{60}^+ and ~ 8.5 eV for C_{52}^+ - C_{58}^+ [15]) the C_{60}^+ ion should be excited to the energies at least ~ 10 eV to emit C_2. Because the normal energy is not dissipated, the origin of the internal excitation is the parallel energy of the projectile C_{60}^+ ion.

The energy $E(C_{60}^+)$ of the parent C_{60}^+ ion which become C_{60-2n}^+ ion via C_2-loss can be estimated with the observed energy $E(C_{60-2n}^+)$ of C_{60-2n}^+ ion by $E(C_{60}^+) = E(C_{60-2n}^+)\times 60/(60-2n)$. Figure 6 shows examples of the estimated energy spectra of the parent C_{60}^+ ions which were detected as C_{60-2n}^+ ions after C_2-losses. The energy of the ion decreases with decreasing size of the cluster. This means that the C_{60}^+ ions which lost larger parallel energy emit more C_2 molecules. The present result clearly indicates that the parallel energy is transferred to the internal excitation of C_{60}^+. The energy losses for C_{60-2n}^+ ions are shown in Fig. 7 as a function of θ_i. The energy loss increases with θ_i and the energy loss difference between the adjacent peaks (~ 7 eV) is almost independent of either θ_i or the size of the cluster.

The C_2 emission probabilities of excited C_{60-2n}^+ ions can be calculated using the emission rate

$$k(C_{60-2n}^+) = A(C_{60-2n}^+)\times \exp\left(-\frac{E_d(C_{60-2n}^+)}{k_B T_e}\right), \qquad (1)$$

where $E_d(C_{60-2n}^+)$ is the dissociation energy for C_2 loss and T_e is the emission temperature of C_{60-2n}^+, which can be estimated from the internal energy E_{in} [5]. The probability that the

excited C_{60}^+ ions are observed as C_{60-2n}^+ by the CEA after a series of C_2 loss can be easily calculated by solving simple rate equations. For example, the probability of detection of C_{58}^+ is given by

$$P(C_{58}^+) = \frac{k(C_{60}^+)}{k(C_{60}^+) - k(C_{58}^+)} \left[\exp\left\{ -k(C_{58}^+)(t_1 + t_2) \right\} - \exp\left\{ -k(C_{58}^+)t_2 - k(C_{60}^+)t_1 \right\} \right], \quad (2)$$

where t_1 (= 3.5 μs) and t_2 (= 5.9 μs) are the flight time between the target and the entrance of CEA and that of inside CEA, respectively. We used the values given in the literatures [15, 16] for $A(C_{60-2n}^+)$ and $E_d(C_{60-2n}^+)$. Figure 8 shows the calculated probabilities for C_{60-2n}^+ as a function of the internal energy. The calculated survival probability of C_{60}^+ decreases very rapidly when its internal energy exceeds ~ 38 eV and becomes almost zero at 45 eV. On the other hand, the observed energy loss of C_{60}^+ at θ_i = 4 ° is about 60 eV. If all dissipated parallel energy was transferred to the internal excitations, C_{60}^+ ion cannot survive. This indicates that only a part of the dissipated energy was transferred to the internal energy of C_{60}^+. The rest of the dissipated energy should be transferred to KCl(001). Except for C_{60}^+, the calculated probabilities show a well defined peak. The most probable internal energies of C_{60}^+ ions which were detected as C_{60-2n}^+ after delayed C_2-loss are approximated by these peak energies. The calculated peaks are almost equally separated, which is in agreement with the observed result (see Fig. 7), although the calculated peak separation (8 – 9 eV) is slightly larger than the observed one (~7 eV). In passing we note that the radiative cooling, which was neglected here, is negligibly small in the present case. For example, the radiation cooling rate is estimated to be 0.34 eV/μs even at E_{in} = 60 eV (T_e = 4670 K) [17].

If the internal energy of the incident C_{60}^+ ions is known, the energy transferred from the parallel energy to the internal excitations can be estimated. The internal energy of the incident C_{60}^+ ions can be deduced by measuring the C_{58}^+ fraction in the incident beam. Figure 9 shows the observed energy spectrum of the incident beam. There is a small C_{58}^+ peak at 2.9 keV, which were formed by C_2 loss after the mass separation by the 90º sector magnet. From the observed fraction (6.3×10^{-4}) and the flight time between the magnet and the CEA (112μs), the internal energy of the incident beam is estimated to be 33.4 eV using eq. (1). The estimated internal energy is in good agreement with the value 34.5 eV obtained for

C_{60}^{+} ions produced by ECR ion source [5].

To estimate the average increment of the internal energy, we need the internal energy of the survived C_{60}^{+} ions, $E_{in}(C_{60}^{+})$. The lower and upper bounds of $E_{in}(C_{60}^{+})$ are 33.4 and ~38 eV, respectively. Using these values, the upper and lower bounds of the energy spent for the internal excitations were estimated. Figure 10 shows the result together with the average energy loss of C_{60}^{+} ions during the grazing angle scattering. The fraction of the dissipated parallel energy transferred to the internal excitations is about 10% or less. The main part of the dissipated parallel energy is, therefore, transferred to the KCl(001) surface.

4. Conclusion

We have observed the charge state, angular and energy distributions of reflected particles from a clean KCl(001) surface under grazing angle incidence of 3 keV $C_{60}^{+, 2+}$ ions. The observed charge state distribution shows that C_{60}^{+} is dominant irrespective of the incident charge state. This can be understood by the electronic structures of KCl and C_{60} ions. Both resonant and Auger neutralization processes are prohibited for C_{60}^{+} in front of KCl(001) while effective resonant neutralization of C_{60}^{2+} is allowed. Except for the small angular shift due to the image acceleration, the observed angular distribution has a peak at the specular angle, indicating that the normal energy is not dissipated during the grazing angle scattering. The observed energy spectra, however, show fragmentation of C_{60}^{+} due to C_2 emission. This indicates that a part of parallel energy is transferred to the internal excitations. The internal energy of the scattered C_{60}^{+} ion after the grazing angle scattering is estimated from the observed fragment distribution. The estimated energy which is transferred from the parallel energy to the internal excitations during the grazing angle scattering is about 15 eV at $\theta_i \sim 6$ º and decreases down to almost zero at $\theta_i \sim 1$ º. These energies are less than 10% of the observed energy losses of C_{60}^{+} ions. The main part of the dissipated kinetic energy is transferred to the KCl(001) surface.

Acknowledgement

This work was supported in part by Center of Excellence for Research and Education

on Complex Functional Mechanical Systems (COE program) of the Ministry of Education, Culture, Sports, Science and Technology, Japan.

References

[1] H. Winter, Phys. Rep. **367** (2002) 387.

[2] R. D. Beck, P. St. John, M.M. Alvarez, F. Diederich, and R.L. Whetten, J. Phys. Chem. **95** (1991) 8402.

[3] T. Fiegele, O. Echt, F. Biasiolo, C. Mair, and T.D. Märk, Chem. Phys. Lett., **316** (2000) 387.

[4] R.T. Chancey, L. Oddershede, F.E. Harris, and J.R. Sabin, Phys. Rev. A **67** (2003) 043203.

[5] S. Wethekam and H. Winter, Phys. Rev. A **76** (2007) 032901.

[6] T. Matsushita, K. Nakajima, M. Suzuki and K. Kimura, Phys. Rev. A **76** (2007) 032903.

[7] M. Prutton, *Surface Physics* (Claredon, Oxford, 1983), p. 9.

[8] K. Kimura, G. Andou and K. Nakajima, Phys. Rev. Lett. **81**, 5438 (1998).

[9] S. Tamehiro, T. Matsushita, K. Nakajima, M. Suzuki, and K. Kimura, Nucl. Instrum. Methods Phys. Res., B **256** (2007) 16.

[10] H. Winter, Prog. Surf. Sci. **63** (2000) 177.

[11] S. Wethekam, H. Winter, H. Cederquist and H. Zettergren, Phys. Rev. Lett. **99** (2007) 037601.

[12] M. Hillenkamp, J. Pfister, M.M. Kappes, R.P. Webb, J. Chem. Phys. **111** (1999) 10303.

[13] Y. H. Ohtsuki, K. Koyama, and Y. Yamamura, Phys. Rev. B **20** (1979) 5044.

[14] K. Kimura, M. Hasegawa, and M.H. Mannami, Phys. Rev. B **36** (1987) 7.

[15] B. Concina, S. Tomita, J.U. Andersen, and P. Hvelplund, Eur. Phys. J. D. **34** (2005) 191.

[16] B. Concina, S. Tomita, N. Takahashi, T. Kodama, S. Suzuki, K. Kikuchi, Y. Achiba, A. Gromov, J.U. Andersen, and P. Hvelplund, Int. J. Mass. Spectrom. **252** (2006) 96.

[17] S. Tomita, J. U. Andersen, H. Hansen, P. Hvelplund, Chem. Phys. Lett. **382** (2003) 120.

Figure captions

Fig. 1 Observed angular distribution of reflected particles when 3 keV C_{60}^{+} ions are incident onto KCl(001) at $\theta_i = 2$ °.

Fig. 2 Observed C_{60}^{+} fraction as a function of θ_i. Results for 3-keV C_{60}^{+} incidence (solid circles) and 3-keV C_{60}^{2+} incidence (open circles) are shown.

Fig. 3 Most probable scattering angle of reflected ions (open circles) and neutral particles (solid circles) when 3 keV C_{60}^{+} ions are incident onto KCl(001). The results for 3-keV C_{60}^{2+} incidence are also shown.

Fig. 4 Examples of the observed energy spectra of reflected ions when 3 keV C_{60}^{+} ions are incident onto a KCl(001) surface under grazing incidence. A multi-peak structure is clearly seen at larger θ_i.

Fig. 5 Examples of the observed energy spectra of reflected ions for 1 and 2 keV C_{60}^{+} incidence.

Fig. 6 Energy spectra of the C_{60}^{+} parent ions which were detected as C_{60-2n}^{+} ions after C_2 loss (see text).

Fig. 7 Most probable energy losses of the C_{60}^{+} parent ions which were detected as C_{60-2n}^{+} ions after C_2 loss. The lines through the data points guide the eye.

Fig. 8 The calculated probabilities that excited C_{60}^{+} ions are observed as C_{60-2n}^{+} by the CEA after a series of C_2 loss.

Fig. 9 Observed energy spectrum of the incident C_{60}^{+} beam. There is a small peak corresponding to C_{58}^{+} ions which were produced by C_2 loss in the beam line after mass

separation.

Fig. 10 Estimated energy which are transferred from the parallel energy to the internal excitations during the reflection of 3 keV C_{60}^{+}. Observed average energy losses of the reflected C_{60}^{+} ions are also shown for comparison.

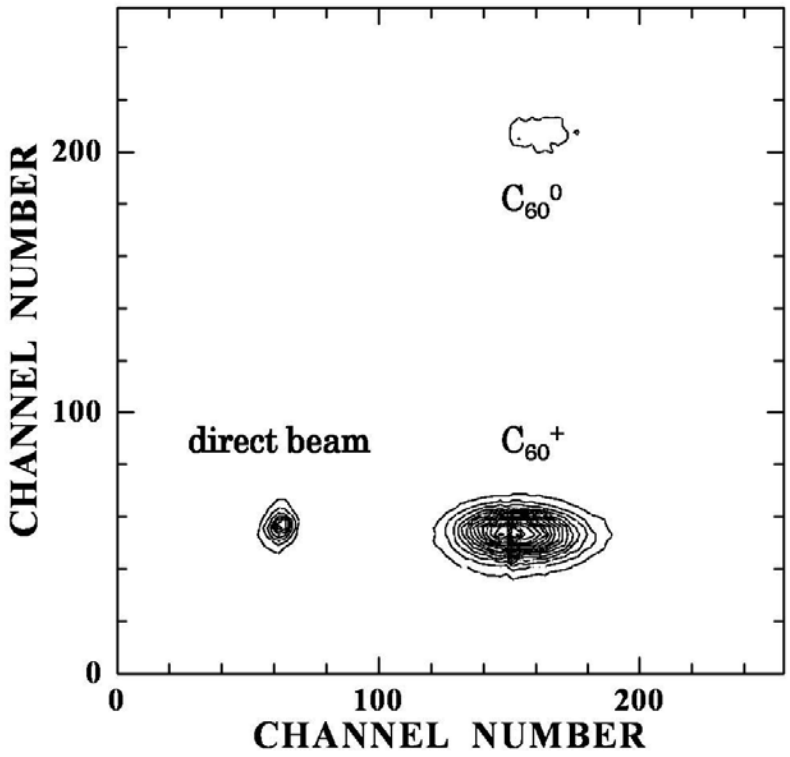

Fig. 1 K. Kimura et al

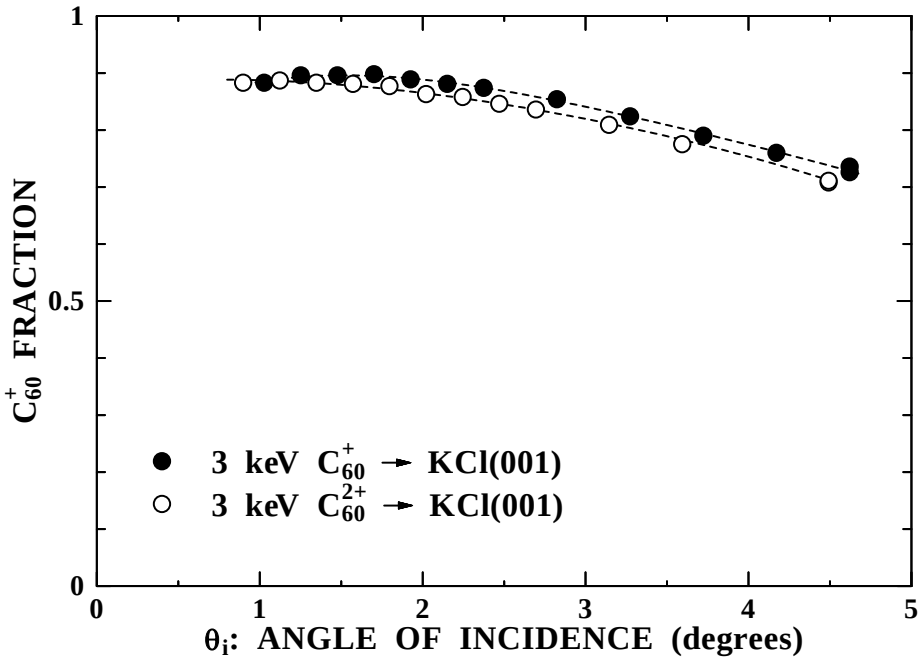

Fig. 2 K. Kimura et al

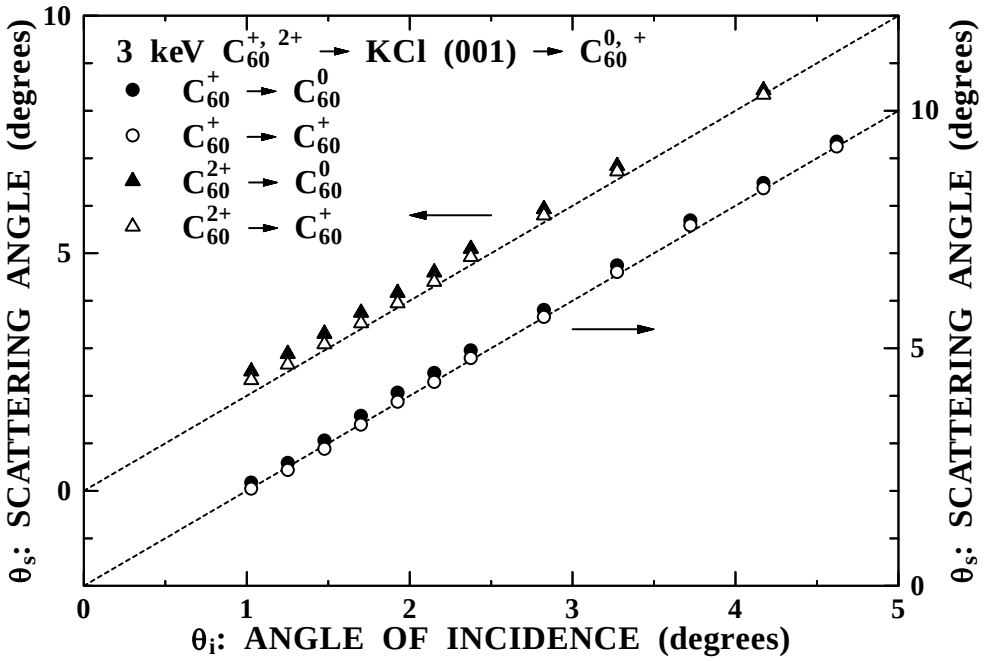

Fig. 3 K. Kimura et al

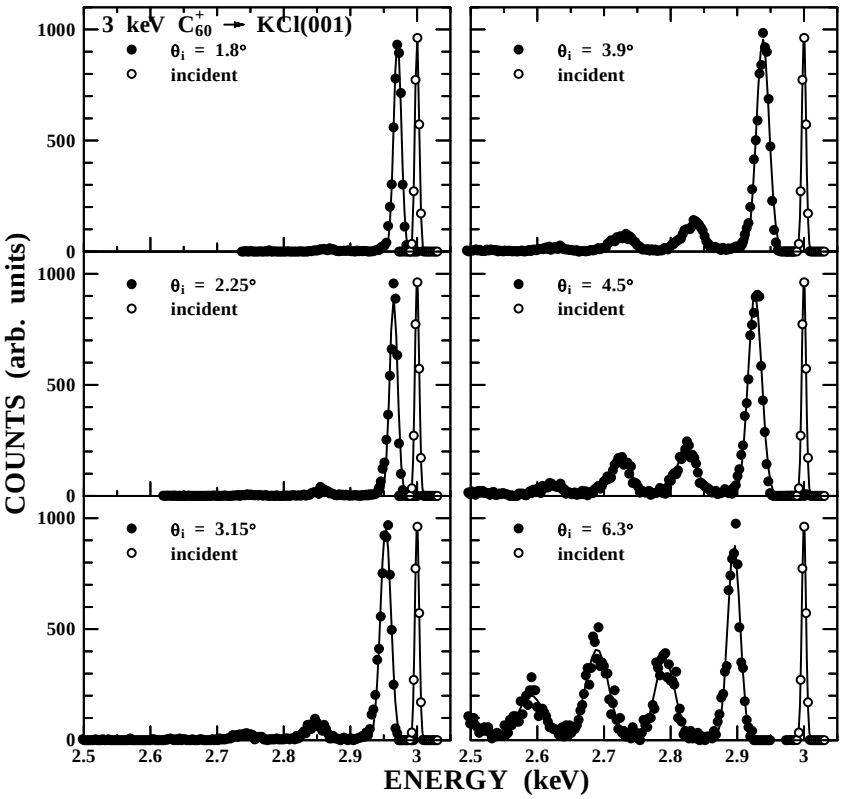

Fig. 4 K. Kimura et al

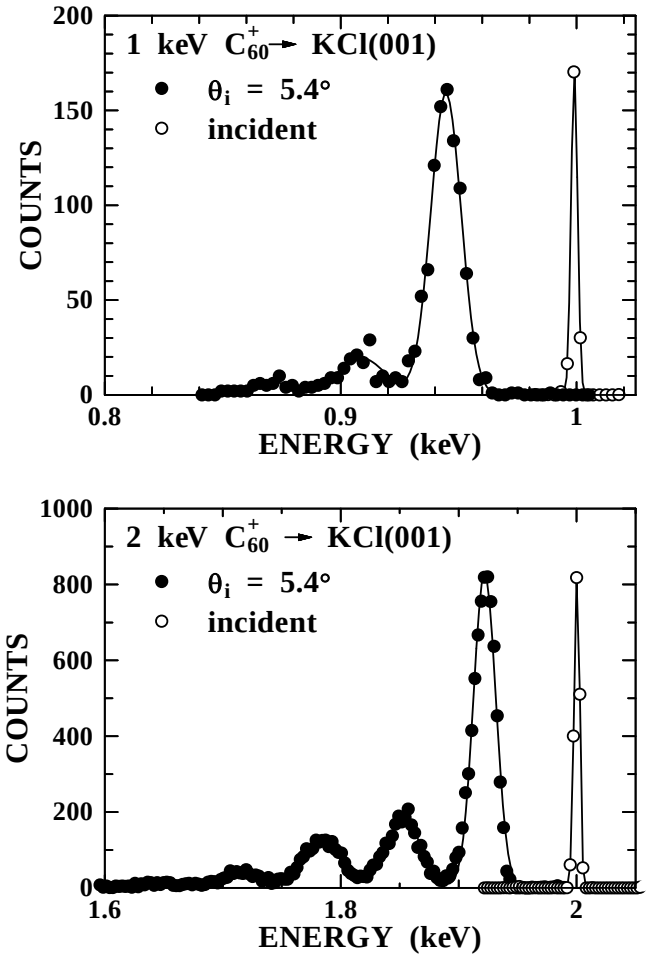

Fig.5 K. Kimura et al

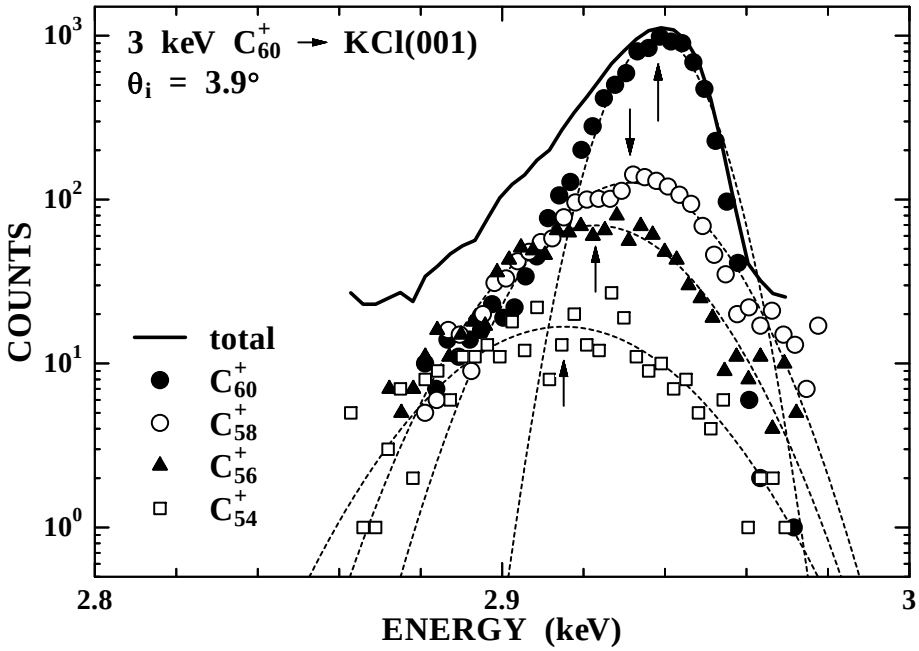

Fig. 6 K. Kimura et al

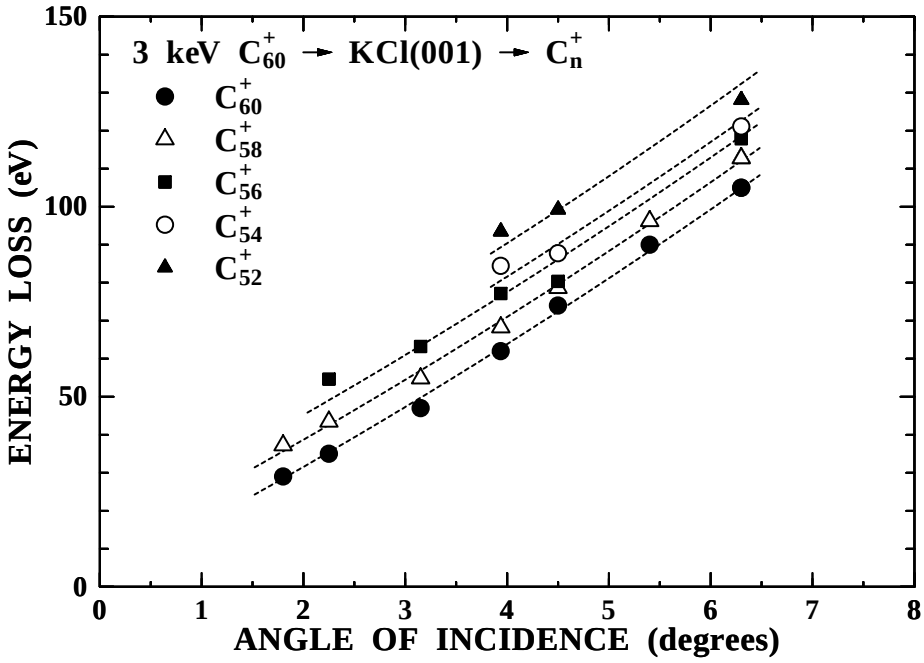

Fig. 7 K. Kimura et al

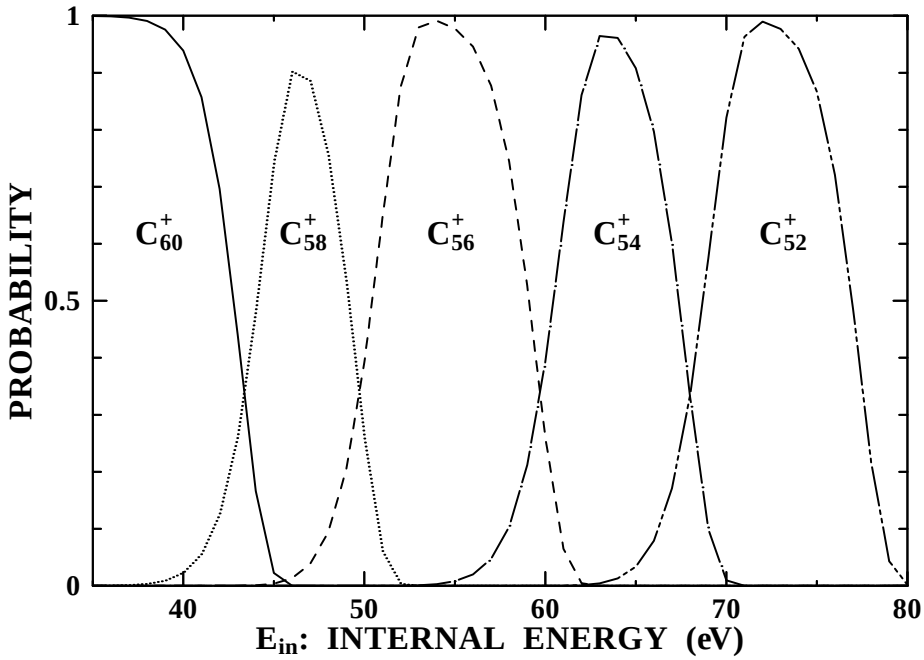

Fig. 8 K. Kimura et al

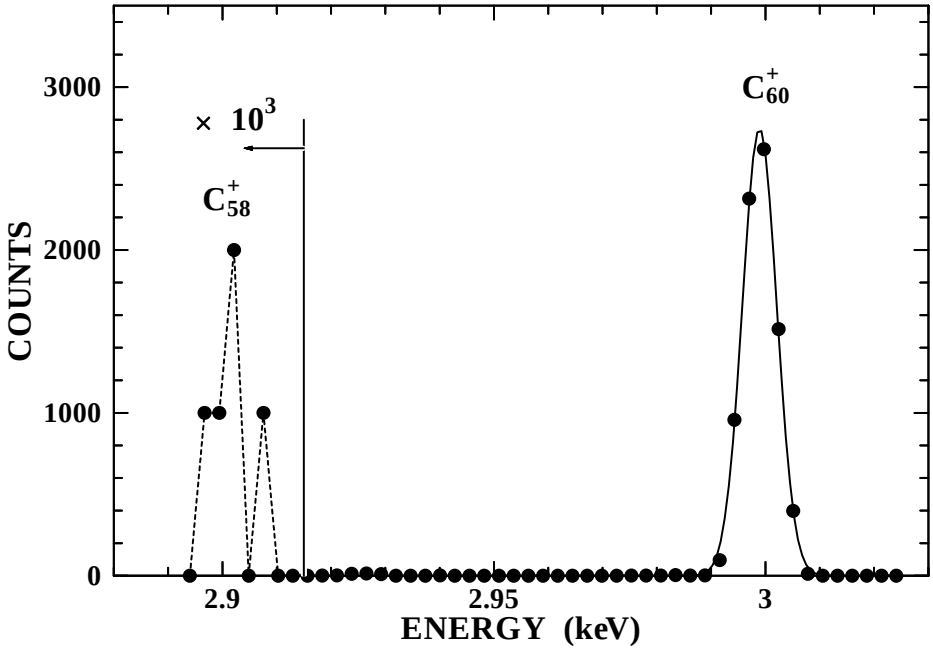

Fig. 9 K. Kimura et al

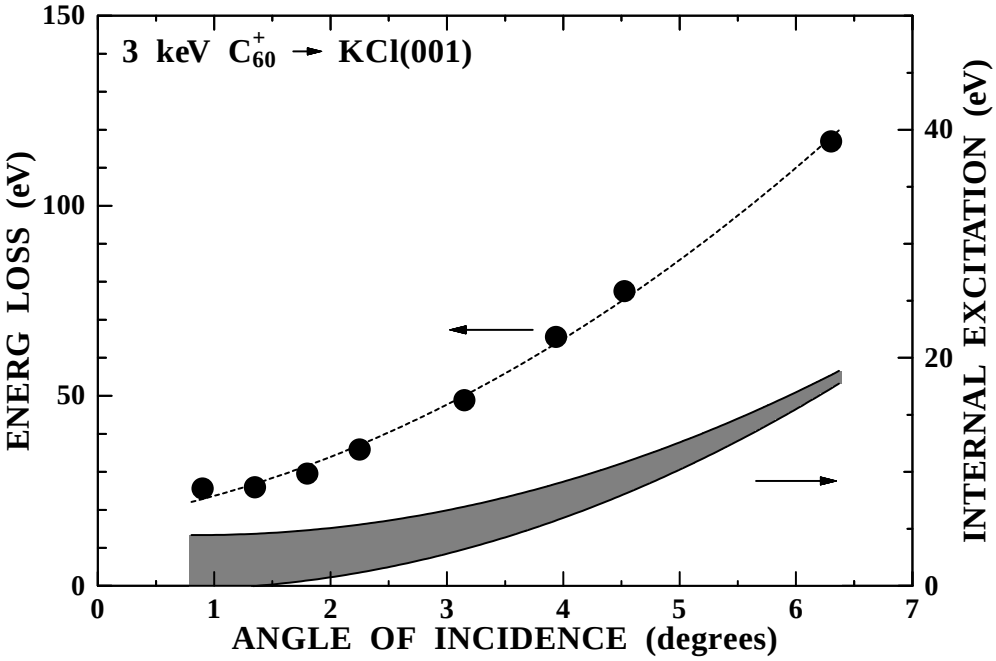

Fig. 10 K. Kimura et al